

Cite this: *Mater. Adv.*, 2023,  
4, 3292

# Oriented quasi-domain structure of helical spin polymers prepared by electrochemical polymerization in a cholesteric liquid crystal under a magnetic field, showing a helical stripe magnetic domain†

Masashi Otaki,<sup>a</sup> Shigeki Nimori<sup>b</sup> and Hiromasa Goto \*<sup>a</sup>

We report the synthesis and alignment of organic radicals with helical structures. Helical spin  $\pi$ -conjugated polymers bearing organic radicals were synthesized by electrochemical polymerization in cholesteric liquid crystals under a magnetic field, using several types of oligothiophenes containing phenoxy radicals in the side chain as the monomers. Under the magnetic field, the polymerization proceeded in the helical liquid crystal matrix oriented in the direction of the magnetic field. These polymers were aligned with its helical axis perpendicular to a magnetic field of 6.0 T. In addition, electrochemical measurements showed that phenoxy radicals in the side chain and polarons as charge carriers in the main chain were respectively produced. The phenoxy radical with a  $g$  value of 2.00415 was confirmed from the electron spin resonance spectroscopy measurements. Superconducting quantum interference device magnetometry measurements revealed that these polymers thus obtained are paramagnetic materials. The optical texture and magnetic spectroscopy measurements indicate that the films thus prepared are helical spin polymers with an oriented quasi-domain structure, showing magneto-electro-optical activity. The optical texture corresponds to the helical stripe magnetic domain of the polymer. This method provides a novel approach for the fabrication of chiral magnets and molecular spin electronics.

Received 8th April 2023,  
Accepted 19th May 2023

DOI: 10.1039/d3ma00161j

rsc.li/materials-advances

## 1. Introduction

Organic molecular materials are lightweight and flexible, allowing for simple film formation processes. In addition, the molecules can self-assemble, enabling a bottom-up approach to manipulate molecular alignment and processing.<sup>1–4</sup> As a kind of self-organized mesophase material, liquid crystals (LCs) exhibit fluidity, diamagnetic anisotropy, and good response to external force fields such as magnetic fields.<sup>5–8</sup> In previous studies, the magnetic field-induced orientation of LC  $\pi$ -conjugated polymers was realized; however, this macroscopic orientation requires high temperatures ( $>100$  °C) and long reaction times due to the high viscosity of the polymers.<sup>9</sup>

Recently, LCs have been used as a template for polymer orientation. For instance, electrochemical polymerization in an

LC electrolyte solution was performed<sup>10</sup> using nematic LC, smectic A LC, and cholesteric LC (CLC) reaction media.<sup>11–13</sup> CLCs are chiral LCs that have one-handed macroscopic helical structures with a twist axis perpendicular to the local director.<sup>14,15</sup> Our group has developed an electrochemical polymerization method in LCs. The electrochemical polymerization in CLC affords  $\pi$ -conjugated polymer films with CLC-like helical morphologies and optical activity owing to the transfer of chirality from the CLC, which enables the synthesis of chiral polymers from achiral monomers. The addition of chirality to conjugated polymers is an essential strategy for developing applications such as circularly polarized luminescence (CPL) materials.<sup>16–22</sup> Furthermore, electrochemical polymerization in LCs under a magnetic field at room temperature allows anisotropic growth of conjugated backbones aligned along the direction of the LC media.<sup>23–26</sup> In CLC, the helical axis is aligned perpendicular or parallel to the direction of the magnetic field. These conjugated polymers thus obtained exhibit polarized absorption with macroscopic orientation.

Currently, such conjugated polymers receive considerable research attention owing to their characteristic optical,

<sup>a</sup> Department of Materials Science, Faculty of Pure and Applied Sciences, University of Tsukuba, Tsukuba, Ibaraki 305-8573, Japan. E-mail: gotoh@ims.tsukuba.ac.jp

<sup>b</sup> National Institute for Materials Science, Tsukuba, Ibaraki, 305-0003, Japan

† Electronic supplementary information (ESI) available. See DOI: <https://doi.org/10.1039/d3ma00161j>



electrochemical, and magnetic properties, all of which can be modulated by rationally designing and controlling the polymer structure. Particularly, organic magnets consisting of  $\pi$ -conjugated materials have been proposed as the next generation of synthetic metals. To stabilize high-spin states, approaches for spin alignment *via* intramolecular bonds on the  $\pi$ -conjugated backbone have been studied. Nishide *et al.* investigated extensively a series of polyacetylene-,<sup>27,28</sup> polyphenylenevinylene-,<sup>29–31</sup> and polythiophene-<sup>32,33</sup> based polyradicals. According to these reports, polymers exhibiting ferromagnetic-like intramolecular spin alignment were synthesized, and the formation of planar and crosslinked polyradical frameworks on  $\pi$ -conjugated backbones was considered an important factor for spin parallel alignment. Recently, stable organic semiconductors with a high-spin state were synthesized using benzobisthiadiazole-based donor–acceptor conjugated polymers.<sup>34–36</sup> By utilizing an appropriate molecular design to reduce the energy gap between the highest occupied molecular orbital and the lowest unoccupied molecular orbital, stable open-shell diradical properties can be induced, enabling easy magnetic switching from a low-spin ground state to a high-spin ground state and intermolecular ferromagnetic diradical coupling. Furthermore, Swager *et al.* reported the preparation of 1,3-bisdiphenylene-2-phenylallyl-based  $\pi$ -conjugated radical polymers as magneto-optic materials with intense Faraday rotations as a new strategy for the development and application of organic magnets.<sup>37–39</sup>

Although the induction of magnetism *via* intramolecular spin alignment has been reported, spin alignment generated by macroscopic intermolecular ordering is still scarce. Recently, a spin arrangement along the macroscopic orientation of an LC was achieved by producing supramolecules containing organic radicals in a magnetic field-oriented LC.<sup>40,41</sup> In our group, a chiral magnetic conjugated polymer was synthesized.<sup>42,43</sup> The study aimed to synthesize a conjugated polymer with macroscopic orientation in one direction by performing electrochemical polymerization in an LC, which enables molecular assembly orientation, under a magnetic field.

In the present study, three types of oligothiophenes bearing a 2,6-di-*tert*-butyl phenol side group as a precursor of the stable radical are synthesized. Next, optically active polymer films are prepared in a CLC under the magnetic field followed by oxidation for the generation of helical spins. The helical axis of the main chain and the degree of orientation can be determined by linearly polarized UV–vis absorption spectroscopy (LPUV–vis) measurements. The magnetic properties of these polymers are investigated by electron spin resonance (ESR) and superconducting quantum interference device (SQUID) magnetometry.

CLCs form a quasi-domain structure like the smectic state observed in the formation of fan-shaped textures. The polymer prepared in a CLC exhibits a pattern of helical magnetic domains like that observed for inorganic magnets (Fe<sub>0.5</sub>Co<sub>0.5</sub>Si) by Lorentz electron microscopy.<sup>44</sup> The polymers prepared in this study imprint a unidirectionally oriented CLC structure and can exhibit a paramagnetic or antiferromagnetic quasi-domain structure.

## 2. Experimental

### 2.1. Materials and methods

The commercially available reagents were received from Nacal Tesque (Kyoto, Japan), Sigma-Aldrich (St. Louis, USA), Kanto Chemical Industry (Tokyo, Japan), and Tokyo Chemical Industry (TCI) (Tokyo, Japan) and used without further purification.

<sup>1</sup>H nuclear magnetic resonance (NMR) spectra were recorded on a JNM-ECS 400 MHz spectrometer (JEOL, Akishima, Japan). All signals were reported in ppm with the internal TMS (tetramethylsilane) signal at 0.00 ppm or CHCl<sub>3</sub> at 7.26 ppm as a standard. <sup>1</sup>H NMR data were recorded as follows: chemical shift ( $\delta$ , ppm), multiplicity (s = singlet, d = doublet, t = triplet, quint = quintuplet, sext = sextuplet, m = multiplet), coupling constant in Hz, integration. Infrared spectra were recorded on a Fourier transform infrared spectrometer (FT-IR)-500 using KBr powder (JASCO, Tokyo, Japan). Frequencies are given in reciprocal centimeters (cm<sup>-1</sup>) and absorbances are recorded. Magnetic orientation was carried out with a drum-type cryogen-free superconducting magnet (Japan Magnet Technology, JMT, Kobe, Japan). UV–vis absorption spectra were obtained using a JASCO V-630 UV–vis spectrophotometer. Circular dichroism (CD) absorption for the polymers was performed using a JASCO J-720 spectrometer. Electrochemical measurements of polymers were conducted using electrochemical analyzer ( $\mu$ Autolab III, Autolab, The Netherlands). The cyclic voltammetry (CV) measurements with these polymer films on indium tin oxide (ITO)-coated glass were conducted using 0.1 M tetrabutylammonium perchlorate (TBAP) in acetonitrile (ACN) as an electrode, Ag/Ag<sup>+</sup> as the reference electrode, and Pt wire as the counter electrode. Ferrocene ( $E_{1/2} = 0.20$  V) was used as an external standard. Magnetic susceptibility measurements of the polymer were carried out using SQUID (Quantum Design CA, magnetic property measurement system, MPMS). ESR measurements were conducted using a JEOL JES TE-200 spectrometer with 100 kHz modulation (X-band).

### 2.2. Synthesis of monomers

The following four types of monomers were synthesized in this paper: (1) 3-(3,5-di-*tert*-butyl-4-hydroxyphenyl)thiophene (1TP) is a mono thiophene bearing a 2,6-di-*tert*-butyl phenol substituent as a side group; (2) 3''-(3,5-di-*tert*-butyl-4-phenoxy)-2,2':5',2'':5'',2''':5'''-quinquethiophene (5TP) is a thiophene pentamer bearing a 2,6-di-*tert*-butyl phenol substituent as a side group and adopts a rod-like structure suitable for electrochemical polymerization in LCs; (3) 3'-(3,5-di-*tert*-butyl-4-phenoxy)-2,2':5',2''-terthiophene (3TP) is a thiophene trimer with a shorter conjugation chain than that of 5TP, bearing a 2,6-di-*tert*-butyl phenol substituent as a side group; and (4) 3''-(3,5-di-*tert*-butyl-phenyl)-2,2':5',2'':5'',2''':5'''-quinquethiophene (5TB) is a thiophene pentamer with a bulky nonradical side group, which was prepared for comparison. 5TB has a structure analogous to that of 5TP but with no phenoxy radicals. Scheme S1 (ESI<sup>†</sup>) illustrates the synthetic route to these monomers. The structures of these monomers were identified by <sup>1</sup>H NMR and FT-IR spectroscopies (Fig. S1–S14, ESI<sup>†</sup>). In the FT-IR spectra of 1TP, 3TP, and 5TP, the signal derived from the



OH substituent appeared at  $3618\text{ cm}^{-1}$  as a sharp band due to the absence of hydrogen bonding (Fig. S15, ESI<sup>†</sup>). As expected, the spectrum of 5TB showed no signal attributable to OH stretching. In addition, an absorption derived from the side chain methyl group common to the three monomers was observed at  $2956\text{ cm}^{-1}$ . Thus, the  $^1\text{H NMR}$  and FT-IR spectra confirmed the successful synthesis of 1TP, 3TP, 5TP, and 5TB.

### 2.3. Synthesis of polymers

Next, 1TP, 3TP, 5TP, and 5TB were used as monomers for the electrochemical polymerization in CLCs. To prepare a CLC, 4-cyano-4'-pentylbiphenyl (5CB), which is a nematic LC at  $25\text{ }^\circ\text{C}$ , was used as an achiral LC matrix, *i.e.*, the host LC. The addition of chiral compounds to such matrices produces CLCs, which are chiral versions of the nematic LCs. In the present study, cholesteryl pelargonate was used as a chiral dopant to induce the formation of a helical structure. The constituents of the electrolytic CLC solution for the electrochemical polymerization of the monomers are summarized in Table 1. The electrolytic CLC solution was prepared by adding the monomer (5TP or 5TB) and TBAP as a supporting salt to the CLC solution. This electrolytic CLC solution was injected between two ITO-coated glass electrodes as an anode and a cathode, respectively, which were separated by a poly(tetrafluoroethylene) spacer of  $200\text{ }\mu\text{m}$  thickness (Fig. 1a). In the electrolytic cell, the helical axes of the CLCs were arranged parallel to the substrate electrodes. The polarizing optical microscopy (POM) image

shown in Fig. 2a confirmed the CLC phase-like fingerprint pattern of the electrolytic solution at  $25\text{ }^\circ\text{C}$ . The monomers in the ITO-coated glass electrodes containing the electrolytic CLC solution were then electropolymerized under a magnetic field (Fig. 1b).

The electrochemical polymerization was performed by applying a constant  $4.0\text{ V DC}$  voltage to the sandwiched cell for  $30\text{ min}$ . After the polymerization, the remaining CLC solution was removed by washing with *n*-hexane to produce the desired polymeric thin film on the anodic surface (Fig. 1c). The polymer films obtained from the three monomers under zero magnetic field were named p5TP<sub>(OT)</sub>, p5TB<sub>(OT)</sub>, and p3TP<sub>(OT)</sub>, respectively. 1TP formed no electrolytically polymerized films. This is because the thiophene moiety of 1TP has lower linearity in the form and low electro-polymerization activity compared to other monomers such as 3TP, 5TP, and 5TB.

Previously, using another conjugated monomer species for electrochemical polymerization in an LC under a magnetic field, the most uniaxially oriented film was obtained with a magnetic flux density of  $4.5\text{ T}$ .<sup>45,46</sup> Therefore, to select the optimal conditions, the present polymerization method was performed under a magnetic field of  $4.0\text{ T}$  or  $6.0\text{ T}$  at  $25\text{ }^\circ\text{C}$ . First, the polymerization cell was heated to obtain an isotropic phase and quickly placed in a drum-type magnetic chamber. The magnetic alignment was conducted for  $30\text{ min}$  in the presence of the magnetic field before performing the polymerization,

Table 1 Constituents of the electrolyte CLC solutions

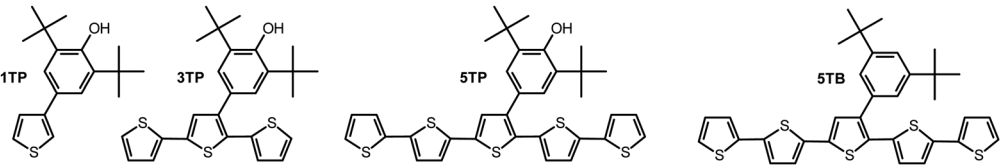
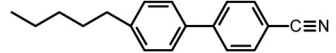
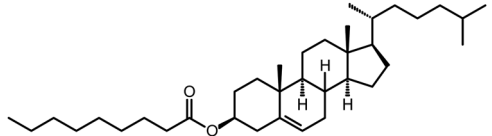
Constituents	Chemical structure	wt%
Monomers		0.475
Nematic LC		95.0
Chiral inducer		4.29
Supporting salt	(C <sub>4</sub> H <sub>9</sub> ) <sub>4</sub> NClO <sub>4</sub> Tetrabutylammonium perchlorate	0.235



Fig. 1 Sandwich cell electrochemical polymerization in a liquid crystal under a magnetic field, and electrochemical polymerization in a CLC medium with transcription of its helical structure. CLC: cholesteric liquid crystal.



while the isotropic phase changed to the CLC phase. Then, a constant DC voltage of 4.0 V was applied to the cell for 30 min to perform the electrochemical polymerization under a magnetic field of 4.0 T or 6.0 T (Fig. 1b). After the polymerization, the mixture was treated as mentioned above for the samples obtained under zero magnetic field. The polymer films synthesized under a magnetic field of 4.0 T or 6.0 T were named p5TP<sub>(4T, 6T)</sub>, p5TB<sub>(4T, 6T)</sub>, and p3TP<sub>(4T, 6T)</sub>, respectively.

### 3. Results and discussion

#### 3.1. Transcription of the CLC structure

The surface structures of the resultant polymeric thin films were observed by the POM. Under zero magnetic field, the p5TP<sub>(0T)</sub>, p5TB<sub>(0T)</sub>, and p3TP<sub>(0T)</sub> polymer films exhibited a fingerprint-like texture with labyrinth-like stripes, indicating the occurrence of the transcription from the helical continuum of the CLC to the polymer (Fig. 2b), which was confirmed by performing CD and UV-vis optical absorption spectroscopy measurements of the polymer films after reduction with hydrazine vapor (Fig. S16, ESI<sup>†</sup>).

In contrast to these polymers obtained under zero magnetic field, the polymer films synthesized *via* magnetic alignment at

an appropriate magnetic flux density showed a linearly striped pattern parallel to the magnetic field, in which the conjugated polymer stands perpendicular to the substrate (black stripes) and the distance between adjacent black stripes is half the spiral pitch. When the electrochemical polymerization was performed under a magnetic field of 4.0 T using 5TP (Fig. 2c) and 5TB (Fig. S17a, ESI<sup>†</sup>) as monomers, a striped pattern parallel to the magnetic field was also observed. However, no striped pattern was formed under a magnetic field of 6.0 T using either 5TP or 5TB (Fig. S17c and d, ESI<sup>†</sup>) as monomers. The strong magnetic field unwound the helical structure of the CLC, which induced the reversion to the nematic phase. This phenomenon can be defined as magnetic induction for the nematic phase from the CLC. However, this change is no phase transition because the CLC is fundamentally defined as a nematic LC phase. When 3TP was used as the monomer, striped patterns parallel to the magnetic field were obtained at both 4.0 T (Fig. S17b, ESI<sup>†</sup>) and 6.0 T (Fig. 2d). The stripes were derived from the helical periodic structure of the CLC, which indicated that the helical axis was vertically aligned with the magnetic field (Fig. S18, ESI<sup>†</sup>). These results suggest that under magnetic fields of up to 6.0 T, 3TP polymerization proceeds along the CLC orientation direction.

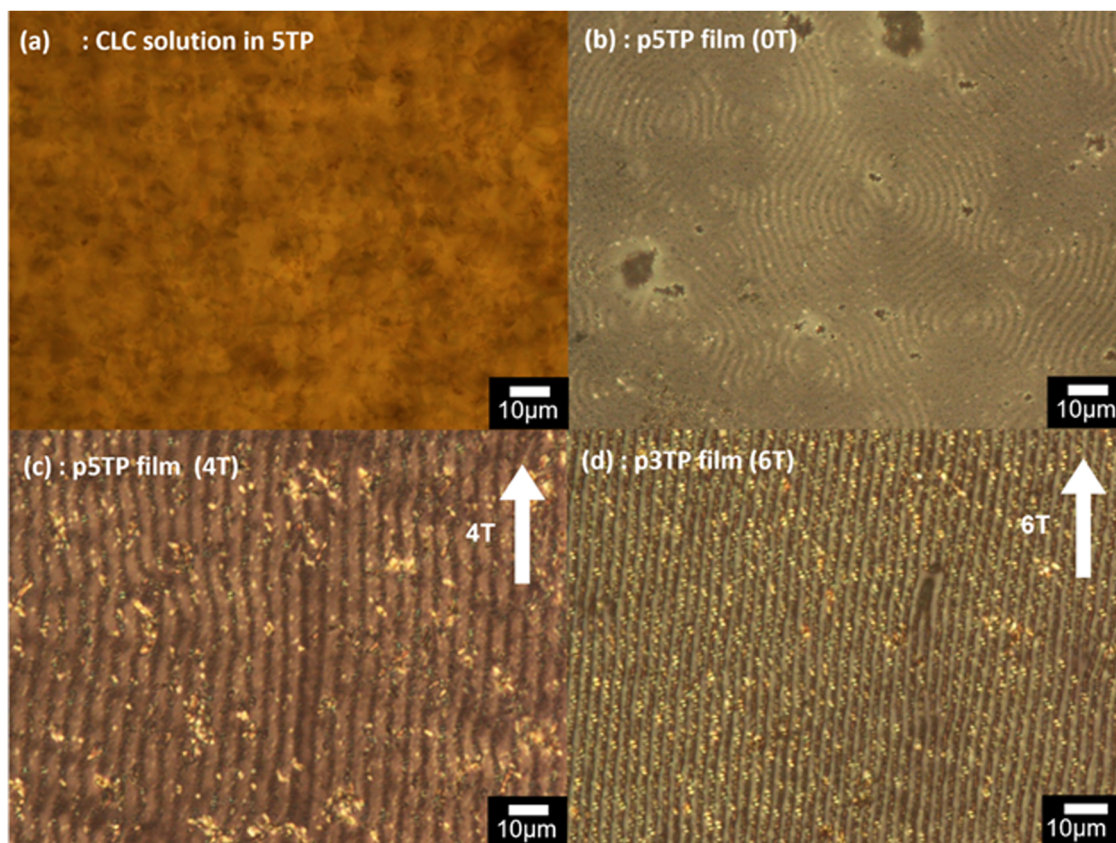


**Fig. 2** Polarizing optical microscopy (POM) images under crossed polarizers of electrochemically prepared polymer films in cholesteric liquid crystal (CLC) under a magnetic field. (a) 5TP prepared in CLC electrolyte under zero magnetic field. p5TP prepared by electrochemical polymerization in the CLC under a magnetic field of (b) 0 T (p5TP<sub>(0T)</sub>) and (c) 4.0 T (p5TP<sub>(4T)</sub>). p3TP prepared by electrochemical polymerization in the CLC under a magnetic field of (d) 6.0 T (p3TP<sub>(6T)</sub>).



### 3.2. Order parameter of the polymer films

The order parameters ( $S$ ) of the polymer films synthesized *via* magnetic alignment were calculated based on LPUV-vis measurement results. The polymer films prepared in the CLC exhibited  $\pi$ - $\pi^*$  transition absorption bands around the UV-vis region. For the polymers prepared under zero magnetic field, the absorption peaks of p5TP<sub>(0T)</sub> and p5TB<sub>(0T)</sub> were observed at around 490 nm, and that of p3TP<sub>(0T)</sub> appeared at 523 nm (Fig. S19, ESI†). However, the absorption peak of the polymers obtained by electrochemical polymerization under a magnetic field appeared blue-shifted. This indicates that the effective conjugated length of the main chain is not extended, and the reactivity is reduced when performing the electrochemical polymerization under the magnetic field. The electrolytic polymer film formed under the magnetic field had a dense structure, and the mobility of the dopant in the film was reduced.<sup>45</sup> The optical absorption wavelength of polymer films prepared under a 6.0 T magnetic field was blue-shifted to *ca.* 50 nm. Then, p5TP<sub>(6T)</sub> and p5TB<sub>(6T)</sub> prepared under a magnetic field of 6.0 T had no stripes, while p3TP<sub>(6T)</sub> maintained the striped structure. Therefore, 3TP having three thiophene rings is suitable as a monomer for electrochemical polymerization in an LC under a magnetic field.

To calculate the degree of orientation of each polymer, the parallel ( $A_{\parallel}$ ) and perpendicular ( $A_{\perp}$ ) polarization absorption spectra of the polymers were measured by LPUV-vis spectroscopy. The order parameter ( $S$ ) of each polymer is summarized in Table 2. The polymer showed stronger absorption in the direction parallel to the magnetic field orientation than in the perpendicular direction. The  $S$  values of the p5TP<sub>(4T)</sub> and p3TP<sub>(4T)</sub> polymers were 0.0267 and 0.0315, respectively, indicating that p3TP has a higher  $S$  than that of p5TP. Furthermore, the  $S$  of p3TP<sub>(6T)</sub> was 0.0629, which was twice the value compared to that of p3TP<sub>(4T)</sub> (Fig. 3a and b). These results suggest that the degree of orientation of the LC phase increased with the magnitude of the magnetic field, and the monomer was polymerized along the direction of the LC orientation.

### 3.3. Electrochemical properties of the polymer films

Electrochemical properties of the polymer films were examined by performing the CV measurements using a monomer-free

**Table 2** Order parameter ( $S$ ) of polymer films synthesized by electrochemical polymerization in CLCs under a magnetic field. The dichroic ratios ( $R$ ) were calculated as  $R = A_{\parallel}/A_{\perp}$ , and  $S = (R - 1)/(R + 2)$

Polymer	Optical texture	Optical absorption peak (nm)	Dichroic ratio ( $R$ )	Order parameter ( $S$ )
p5TP <sub>(0T)</sub>	Fingerprint	488	—	—
p5TP <sub>(4T)</sub>	Stripe	470	1.082	0.0267
p5TP <sub>(6T)</sub>	Isotropic	431	—	—
p5TB <sub>(0T)</sub>	Fingerprint	488	—	—
p5TB <sub>(4T)</sub>	Stripe	476	1.01	0.00341
p5TB <sub>(6T)</sub>	Isotropic	432	—	—
p3TP <sub>(0T)</sub>	Fingerprint	523	—	—
p3TP <sub>(4T)</sub>	Stripe	477	1.098	0.0315
p3TP <sub>(6T)</sub>	Stripe	480	1.201	0.0629

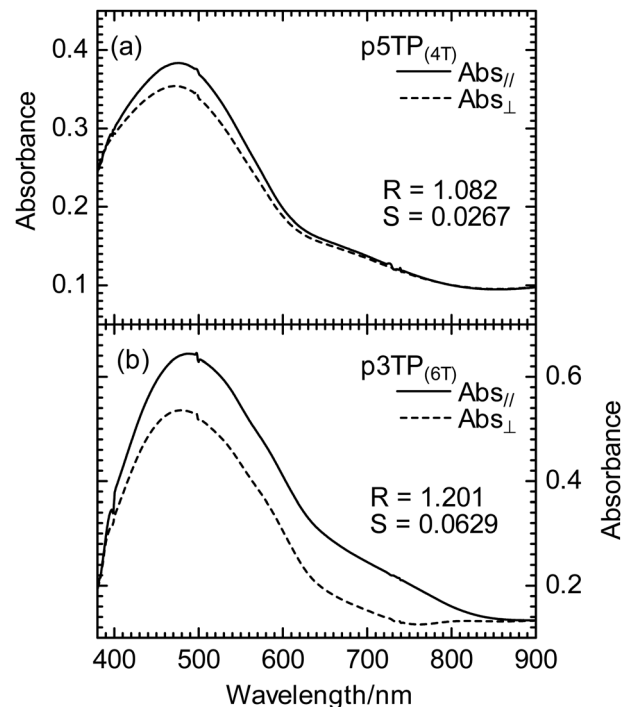


**Fig. 3** Linearly polarized UV-vis absorption spectra of (a) p5TP<sub>(4T)</sub> and (b) p3TP<sub>(6T)</sub> prepared *via* electrochemical polymerization in a CLC under a magnetic field.  $A_{\parallel}$ ,  $A_{\perp}$ : absorbance parallel and perpendicular to the magnetic direction, respectively.

0.1 M TBAP-ACN solution at scan rates of 10–200 mV s<sup>-1</sup> (Fig. S20, ESI†). The potentials were measured relative to an Ag/Ag<sup>+</sup> reference electrode. During the oxidation (doping) process for the p3TP<sub>(0T)</sub> film, an oxidation signal at 0.640 V (scan rate: 10 mV s<sup>-1</sup>) was observed, and its potential gradually increased with the scan rate, reaching 0.879 V at a scan rate of 200 mV s<sup>-1</sup>. During the reduction (dedoping) process for the p3TP<sub>(0T)</sub> film, a reduction signal at 0.514 V (scan rate: 10 mV s<sup>-1</sup>) was observed, and its potential gradually decreased with the scan rate until reaching 0.140 V at a scan rate of 200 mV s<sup>-1</sup>. In addition, the redox properties of the p3TP<sub>(0T)</sub> film were investigated by plotting the intensity of the signal for each scan rate (Fig. S21, ESI†). A linear intensity change of the signal was obtained, which was indicative of the good redox properties of the p3TP<sub>(0T)</sub> film.

The generation of polarons and bipolarons in the p3TP<sub>(0T)</sub> film was confirmed by recording *in situ* ESR spectra during the electrochemical processes at various voltages. Similarly, the ESR spectra in the electrochemical process of p5TP<sub>(0T)</sub> were measured according to a previously reported method.<sup>42</sup> In the oxidation process, the intensity of the ESR signal increased from 0 to 0.4 V with the generation of polarons and then gradually decreased from 0.4 V to 1.0 V as bipolarons (dications) were generated (Fig. 4a). The opposite behavior was observed for the ESR signal in the reduction process (Fig. 4b). The plots of the ESR line width ( $\Delta H_{pp}$ ) and peak-to-peak signal intensity ( $I_{pp}$ ) are shown in Fig. 4c.  $\Delta H_{pp}$  decreased with the generation of polarons up to 0.4 V and then increased due to



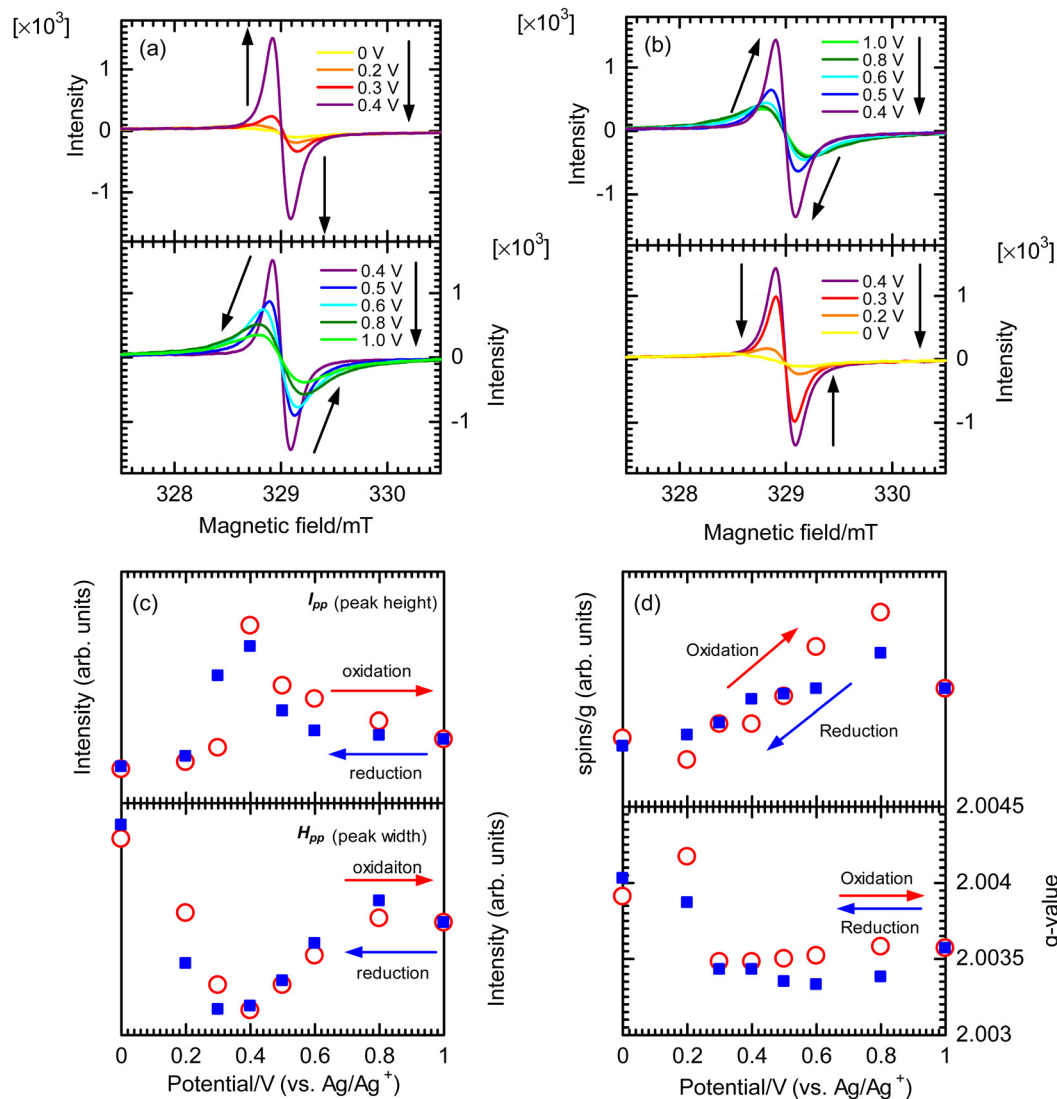


Fig. 4 Electron spin resonance (ESR) data for the p3TP(O7) film during electrochemical oxidation (a) and reduction (b) vs. Ag/Ag<sup>+</sup> at 0.1 V steps. (c) Peak height ( $I_{pp}$ ) and peak width ( $\Delta H_{pp}$ ). (d)  $g$  value and spin concentration.

the generation of bipolarons upon further increasing the voltage up to 1.0 V. The plots of the  $g$  values and the spin concentration are shown in Fig. 4d. The spin concentration increased with the generation of polarons in the main chain. The  $g$  value is indicative of the nature of the radical species of the polymer. At 0.2 V, the  $g$  value was 2.00417 in the oxidation process, which was in good agreement with the  $g$  value of the phenoxy radical. Upon increasing the voltage up to 0.3 V or higher, the  $g$  value became constant at around 2.035, which corresponded to the disappearance of the phenoxy radicals and the production of polarons as charge carriers in the main chain. The selective electrochemical oxidation and generation of phenoxy radicals are possible because the oxidation potential for the generation of phenoxy radicals in the side groups is independent of the generation of polarons in the main chain. This selective electrochemical redox process was also observed for p5TP(O7), which suggests that phenoxy

radicals could be generated exclusively using the specific oxidants.<sup>42</sup>

The generation of polarons and bipolarons was also investigated by *in situ* UV-vis absorption spectroscopy at various voltages using a monomer-free 0.1 M TBAP-ACN solution (Fig. S22, ESI†). Absorption bands were observed at 523, 782, and >1000 nm, which can be assigned to  $\pi-\pi^*$  transitions in the main chain, polarons (radical cations) of the doping band, and bipolarons (dications) of the doping band, respectively. These absorption bands changed as the electrochemical redox process proceeded. Particularly, the band at 523 nm decreased in intensity with increasing voltage, and the polaron and bipolaron bands appeared at long wavelengths. In the reduction process, which is equivalent to electrochemical dedoping, the absorption band at 523 nm increased and the doping bands decreased. Furthermore, this electrochemical doping-dedoping process was repeatable. The color of the

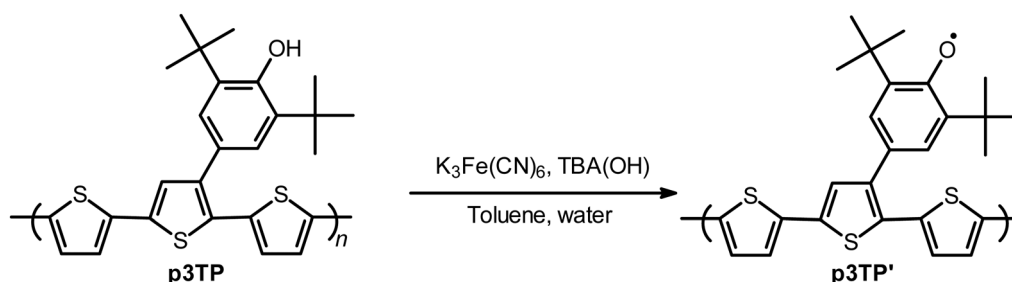


p3TP<sub>(0T)</sub> film changed from red (reduced state) to black (oxidized state) during the electrochemical processes.

### 3.4. Magnetic properties of the polymers

Since the oxidation potentials for the generation of phenoxy radicals and polarons differed within the polymer, the selective chemical oxidation of the OH substituents could be expected to produce phenoxy radicals in the side groups. A previous study reported the selective generation of phenoxy radicals using  $K_3Fe(CN)_6$  as an oxidizing agent.<sup>32</sup> Therefore, this oxidant was

used to perform the selective oxidation of the p3TP film. First, a small amount of tetrabutylammonium hydroxide was added to p3TP<sub>(0T)</sub> in toluene (2 mL), and the solution was stirred for 6 h under a nitrogen atmosphere. Then,  $K_3Fe(CN)_6$  (0.2 g) in water (1 mL) was added to this solution and stirred for 2 h at room temperature. The resultant compound was washed with water three times and dried under reduced pressure to give the desired product p3TP'<sub>(0T)</sub> bearing phenoxy radicals (Scheme 1). Following a similar procedure, phenoxy radicals were generated on the p3TP<sub>(6T)</sub> film, affording p3TP'<sub>(6T-radical)</sub>.



Scheme 1 Synthetic route to p3TP'.  $K_3Fe(CN)_6$ : potassium ferricyanide, TBA(OH): tetrabutylammonium hydroxide.

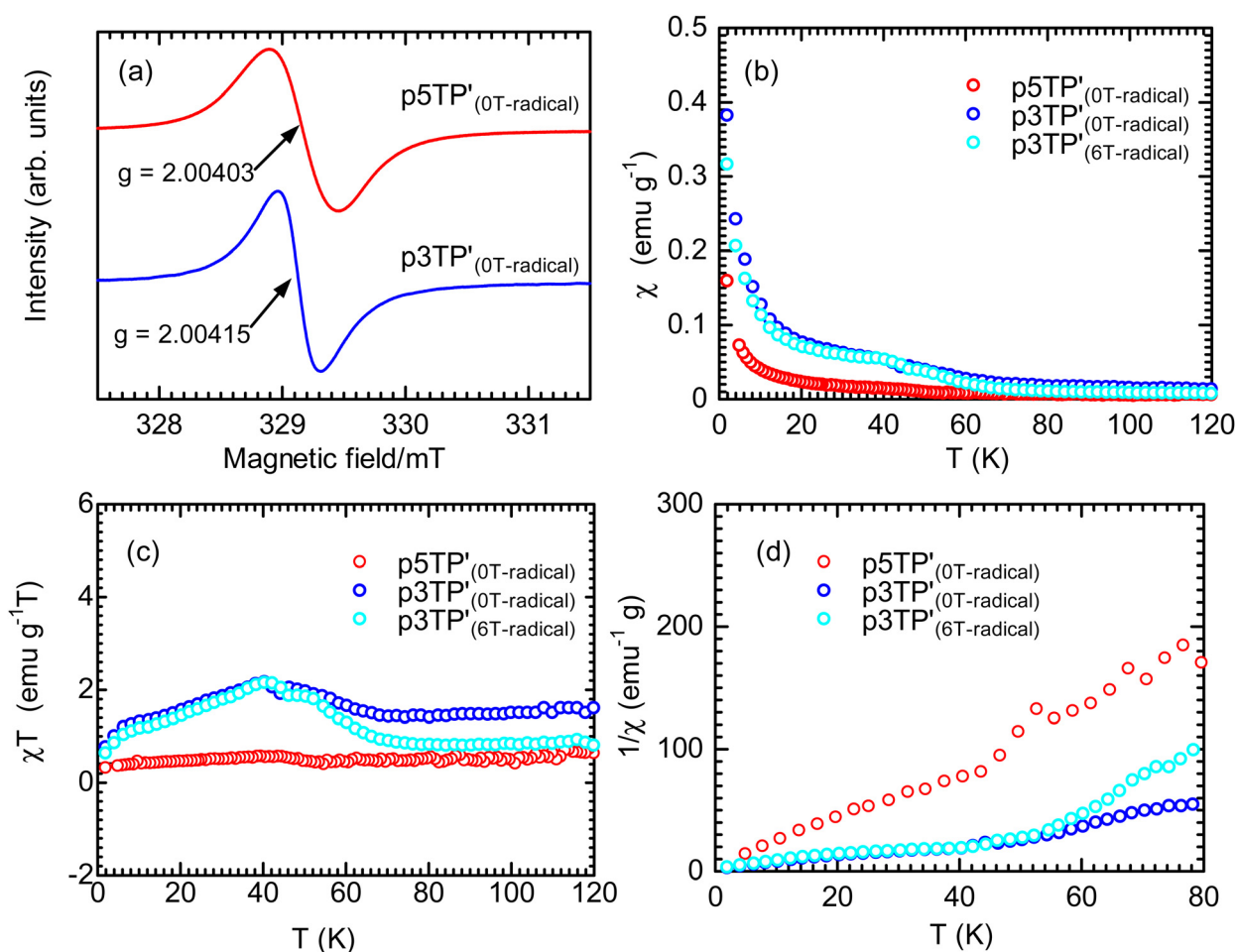


Fig. 5 (a) Electron spin resonance spectra for p5TP'<sub>(0T-radical)</sub> (red line) and p3TP'<sub>(0T-radical)</sub> (blue line). (b)  $\chi$  vs.  $T$  plots, (c)  $\chi T$  vs.  $T$  plots (Curie–Weiss plot,  $C = \chi T$ ), and (d)  $1/\chi$  vs.  $T$  plots for p3TP'<sub>(0T-radical)</sub>, p3TP'<sub>(6T-radical)</sub>, and p5TP'<sub>(0T-radical)</sub>.  $\chi$ : magnetic susceptibility;  $T$ : temperature.



Table 3 Electron spin resonance spectroscopy measurement results

Oxidation methods	Polymer	$\Delta H_{pp}$ (mT)	$g$ value	Spin conc. (spins $g^{-1}$ )
Electrochemical oxidation process	p3TP' <sub>(radical at 0.2 V)</sub>	0.442	2.00417	$0.27 \times 10^{19}$
	p3TP' <sub>(polaron at 0.8 V)</sub>	0.427	2.00350	$0.46 \times 10^{19}$
$K_3Fe(CN)_6$ as an oxidizing agent	p5TP' <sub>(0T-radical)</sub>	0.569	2.00403	$1.53 \times 10^{19}$
	p3TP' <sub>(0T-radical)</sub>	0.362	2.00415	$6.53 \times 10^{19}$
	p3TP' <sub>(6T-radical)</sub>	0.387	2.00410	$3.58 \times 10^{19}$

In the ESR spectrum of the p3TP'<sub>(0T)</sub> film, the  $g$  value of the phenoxy radical (p3TP'<sub>(0T-radical)</sub>) was 2.00415 (Fig. 5a). In the above-mentioned electrochemical redox process, the  $g$  values derived from the phenoxy radical and the polaron (p3TP'<sub>(0T-polaron)</sub>) were 2.00417 and 2.0035, respectively. According to previous reports, the  $g$  value of phenoxy radicals in p5TP'<sub>(0T-radical)</sub> was 2.00403,<sup>42</sup> which confirms the successful generation of phenoxy radicals using  $K_3Fe(CN)_6$  as an oxidizing agent in the present study. In addition, the spin concentration of the p3TP'<sub>(0T)</sub> film was  $6.53 \times 10^{19}$  spin  $g^{-1}$ . The ESR

measurement results of each polymer are summarized in Table 3.

The magnetic susceptibility ( $\chi$ ) of the polymer films was measured using SQUID magnetometry, as shown in Fig. 5b ( $\chi$  vs.  $T$  plots). The  $\chi$  intensity of p3TP'<sub>(0T-radical)</sub> is higher than that of p5TP'<sub>(0T-radical)</sub>, which is attributed to the higher spin concentration of the former polymer than the latter. Meanwhile, the  $\chi$  of p3TP'<sub>(6T-radical)</sub> was lower than that of p3TP'<sub>(0T-radical)</sub>. This is due to the synthesis of p3TP in a magnetic field decreases the effective conjugation length. In addition, the residual oxygen in the samples appeared as weak signals at around 40 K. The  $\chi T$  vs.  $T$

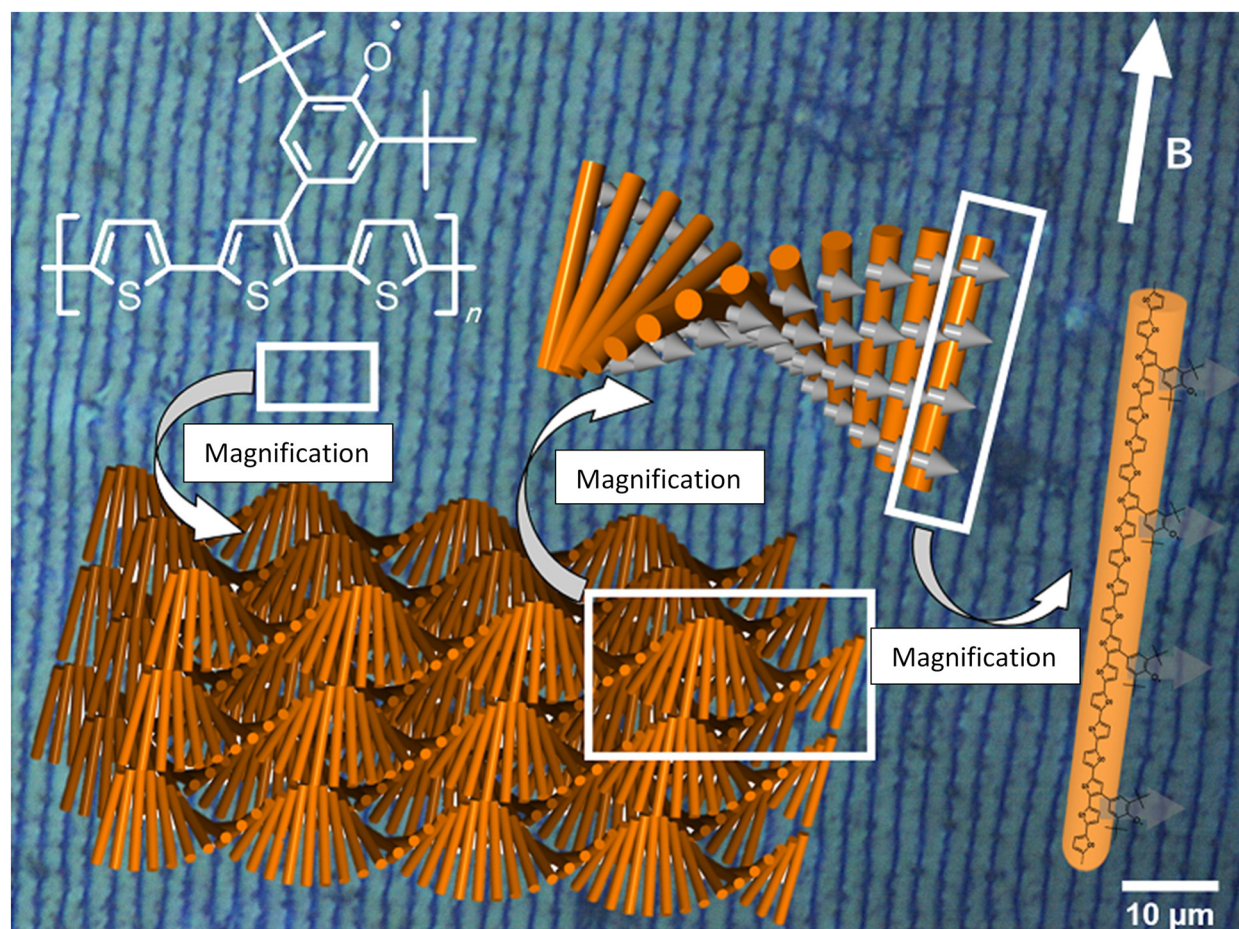


Fig. 6 Plausible structure of the unidirectionally oriented helical polymer p3TP'<sub>(6T-radical)</sub>. The background of this figure is a circularly polarized differential interference contrast optical microscopy image of the polymer showing unidirectional helical stripes obtained by electrochemical polymerization in a liquid crystal under a magnetic field. The orange sticks represent the thiophene backbone of the polymer, and the gray arrows indicate the phenoxy radicals in the polymer side chain. The helical axis of the polymer is perpendicular to the magnetic field direction.





(Curie–Weiss plots) shown in Fig. 5c implies weak antiferromagnetism because the  $\chi T$  value decreased in a low-temperature range, although a clear Néel temperature was not found. These  $1/\chi$  vs.  $T$  curves increased slightly from low to high temperature owing to inter-spin interactions dominating thermal vibrations at low temperature (Fig. 5d). The  $1/\chi$  vs.  $T$  plot indicated that the polymers were paramagnetic or weakly antiferromagnetic, although the low intensity of  $\chi$  makes it difficult to determine a clear inflection point at low temperature. Helical magnets can show paramagnetism or antiferromagnetism.<sup>47</sup> The SQUID results demonstrate that the polymers prepared in this study were magnetically active.

### 3.5. Plausible structure of the polymer film

The polymers obtained from the chiral LC undergo  $\pi$ -stacking with anticlockwise rotation to form a left-handed chiral aggregate as a result of the imprinting of the LC matrix during polymerization. In addition, the LCs are oriented in one direction in a magnetic field, and the conjugated polymers were synthesized along the direction of the LC form stripes. According to these results, it can be concluded that p3TP'<sub>(radical)</sub> exhibits anticlockwise helical spin order and anticlockwise helical aggregation of the main chains. The magneto-optical activity of the p3TP'<sub>(radical)</sub> polymer stems from the hierarchical intramolecular helical spin order and the CLC-like intermolecular 3D helical structure. A plausible structure of the polymer prepared by electrochemical polymerization in CLCs under a magnetic field is shown in Fig. 6. The background of this figure is a circularly polarized differential interference contrast optical microscopy image of the polymer prepared by electrochemical polymerization in CLCs under the magnetic field, showing unidirectional helical stripes. The stripes stem from the helical periodic structure of the CLC, which indicates that the intermolecular helical axis was perpendicularly aligned against the magnetic field. In addition, the helical spins in the main chain form an interhelical structure. The distance between the helical stripes of the fingerprint texture corresponds to the helical half pitch. Further, the mainchain and the spins can form intramainchain helical structure (Fig. S23, ESI†). In this case, a hierarchical helical spin structure is formed.

The polymers synthesized in this study show no ferromagnetic spin alignment because they satisfy no conditions for topological spin parallel alignment at the molecular level required to obtain ferromagnetic order.<sup>48,49</sup> However, a one-handed chiral continuum is formed from the molecular level to macroscopic chiral aggregation with hierarchical intrahelical and interhelical spin order.

## 4. Conclusions

The combination of  $\pi$ -stacking and the rigidity of the conjugated main chain, its chirality, and the stable spin state in the side group afforded polymers exhibiting magneto-, electro-, and optical activity.<sup>40</sup> The resultant polymers form LC-type structures *via* imprinting of the matrix LC without requiring a

mesogen in the polymer. The spin chirality of the polymer is derived from the intra- and inter-helicity of the main chain. In this study, a conjugated polymer macroscopically oriented in one direction was successfully synthesized by performing electrochemical polymerization in CLCs under a magnetic field. The host matrix is a helical LC at room temperature, and the application of a magnetic field causes the monomer to polymerize along the orientation direction of the LC. Observation of the optical texture and magnetic spectroscopy measurements indicate that the films thus prepared are helical spin polymers with an oriented quasi-domain structure, showing magneto-electro-optical activity. The optical texture corresponds to the helical stripe magnetic domain of the polymer. This research demonstrated a new example of the macroscopic orientation of polymer helical spins using a magnetic field.

## Author contributions

Masashi Otaki: methodology, formal analysis, investigation, data curation, visualization, writing – original draft, writing – review & editing. Shigeki Nimori: methodology. Hiromasa Goto: investigation, conceptualization, funding acquisition, methodology, project administration, supervision, writing – review & editing. All authors have read and agreed to the published version of the manuscript.

## Conflicts of interest

The authors declare that they have no known competing financial interests or personal relationships that could have appeared to influence the work reported in this paper.

## Acknowledgements

We would like to thank the OPEN FACILITY, Research Facility Center for Science and Technology, University of Tsukuba, for the use of the NMR and Glass Workshop of University of Tsukuba. This research was supported by the Japan Society for the Promotion of Science (JSPS), Grants-in-Aid for Scientific Research (No. 20K05626, H. Goto).

## References

- H. Hayashi, R. Kikuchi, R. Kumai, M. Takeguchi and H. Goto, Rod-shaped 1D polymer-assisted anisotropic self-assembly of 0D nanoparticles by a solution-drying method, *J. Mater. Chem. C*, 2019, 7, 7442–7453.
- J. Y. Lin, B. Liu, M. N. Yu, X. H. Wang, L. B. Bai, Y. M. Han, C. J. Ou, L. H. Xie, F. Liu, W. S. Zhu, X. W. Zhang, H. F. Ling, P. N. Stavrinou, J. P. Wang, D. D. C. Bradley and W. Huang, Systematic investigation of self-organization behavior in supramolecular  $\pi$ -conjugated polymer for multi-color electroluminescence, *J. Mater. Chem. C*, 2018, 6, 1535–1542.
- Y. J. Heo, J. Kim, H. G. Jeong, S. Y. Jang, H. Hwang, Y. A. Kim, D. H. Lim and D. Y. Kim, Fluorophobic Effect Driven



- Self-Organization of Semifluorinated Alkyl Chain Substituted Conjugated Polymer, *Macromol. Chem. Phys.*, 2017, **218**, 1700176.
- 4 H. Hayashi, T. Iseki, S. Nimori and H. Goto, Vapour-induced liquid crystallinity and self-recovery mechanochromism of helical block copolymer, *Sci. Rep.*, 2017, **7**, 1–8.
  - 5 C. G. Goltner and M. Antonietti, Mesoporous materials by templating of liquid crystalline phases, *Angew. Chem., Int. Ed.*, 1998, **37**, 613–616.
  - 6 M. Andersson, V. Alfredsson, P. Kjellin and A. E. Palmqvist, Macroscopic alignment of silver nanoparticles in reverse hexagonal liquid crystalline templates, *Nano Lett.*, 2002, **2**, 1403–1407.
  - 7 T. Nishimura, T. Ito, Y. Yamamoto, M. Yoshio and T. Kato, Macroscopically Ordered Polymer/CaCO<sub>3</sub> Hybrids Prepared by Using a Liquid-Crystalline Template, *Angew. Chem., Int. Ed.*, 2008, **120**, 2842–2845.
  - 8 M. Yang, Z. Liu, X. Li, Y. Yuan and H. Zhang, Influence of flexible spacer length on self-organization behaviors and photophysical properties of hemiphasmidic liquid crystalline polymers containing cyanostilbene, *Eur. Polym. J.*, 2020, **123**, 109459.
  - 9 H. Goto, S. Nimori and K. Akagi, Synthesis and properties of mono-substituted liquid crystalline polyacetylene derivatives—doping, magnetic orientation, and photo-isomerization, *Synth. Met.*, 2005, **155**, 576.
  - 10 H. Goto, Electrochemical polymerization of pyrrole in cholesteric liquid crystals: Morphology and optical properties, *J. Polym. Sci., Part A: Polym. Chem.*, 2007, **45**, 1377–1387.
  - 11 H. Goto, Doping-dedoping]-driven optic effect of  $\pi$ -conjugated polymers prepared in cholesteric-liquid-crystal electrolytes, *Phys. Rev. Lett.*, 2007, **98**, 253901.
  - 12 H. Yoneyama, K. Kawabata, A. Tsujimoto and H. Goto, Preparation of iridescent-reflective poly (furan-co-phenylene)s by electrochemical polymerization in a cholesteric liquid crystal medium, *Electrochem. Commun.*, 2008, **10**, 965–969.
  - 13 K. Kawabata, M. Takeguchi and H. Goto, Optical activity of heteroaromatic conjugated polymer films prepared by asymmetric electrochemical polymerization in cholesteric liquid crystals: structural function for chiral induction, *Macromolecules*, 2013, **46**(6), 2078–2091.
  - 14 H. Goto, Vortex fibril structure and chiroptical electrochromic effect of optically active poly (3, 4-ethylenedioxythiophene)(PEDOT\*) prepared by chiral transcription electrochemical polymerisation in cholesteric liquid crystal, *J. Mater. Chem.*, 2009, **19**, 4914–4921.
  - 15 H. Kawashima, K. Kawabata and H. Goto, Intramolecular charge transfer (ICT) of a chiroptically active conjugated polymer showing green colour, *J. Mater. Chem. C*, 2015, **3**, 1126–1133.
  - 16 M. Pan, R. Zhao, B. Zhao and J. Deng, Two Chirality Transfer Channels Assist Handedness Inversion and Amplification of Circularly Polarized Luminescence in Chiral Helical Polyacetylene Thin Films, *Macromolecules*, 2021, **54**, 5043–5052.
  - 17 Z. W. Luo, L. Tao, C. L. Zhong, Z. X. Li, K. Lan, Y. Feng, P. Wang and H. L. Xie, High-Efficiency Circularly Polarized Luminescence from Chiral Luminescent Liquid Crystalline Polymers with Aggregation-Induced Emission Properties, *Macromolecules*, 2020, **53**, 9758–9768.
  - 18 X. H. Xu, S. M. Kang, R. T. Gao, N. Liu and Z. Q. Wu, Precise Synthesis of Optically Active and Thermo-degradable Poly (trifluoromethyl methylene) with Circularly Polarized Luminescence, *Angew. Chem., Int. Ed.*, 2023, **62**, e202300882.
  - 19 L. Xu, Y. J. Wu, R. T. Gao, S. Y. Li, N. Liu and Z. Q. Wu, Visible Helicity Induction and Memory in Polyallene toward Circularly Polarized Luminescence, Helicity Discrimination, and Enantiomer Separation, *Angew. Chem., Int. Ed.*, 2023, **62**, e202217234.
  - 20 S. Y. Li, L. Xu, R. T. Gao, Z. Chen, N. Liu and Z. Q. Wu, Advances in circularly polarized luminescence materials based on helical polymers, *J. Mater. Chem. C*, 2023, **11**, 1242–1250.
  - 21 C. Wang, L. Xu, L. Zhou, N. Liu and Z. Q. Wu, Asymmetric Living Supramolecular Polymerization: Precise Fabrication of One-Handed Helical Supramolecular Polymers, *Angew. Chem., Int. Ed.*, 2022, **61**, e202207028.
  - 22 N. Liu, L. Zhou and Z. Q. Wu, Alkyne-palladium (II)-catalyzed living polymerization of isocyanides: an exploration of diverse structures and functions, *Acc. Chem. Res.*, 2021, **54**, 3953–3967.
  - 23 H. Goto and S. Nimori, Liquid crystal electropolymerisation under magnetic field and resultant linear polarised electrochromism, *J. Mater. Chem.*, 2010, **20**, 1891–1898.
  - 24 K. Kawabata, S. Nimori and H. Goto, Horizontal and vertical orientation of polythiophenes by electrochemical polymerization in magnetically aligned smectic liquid crystal, *ACS Macro Lett.*, 2013, **2**, 587–591.
  - 25 H. Hayashi, K. Kawabata, S. Nimori and H. Goto, A Poly-(ter(3,4-ethylenedioxythiophene)) Showing Concentric-circle Morphology Prepared by Electrochemical Synthesis in Smectic A Liquid Crystal under Vertical Strong Magnetic Field, *Chem. Lett.*, 2016, **45**, 170.
  - 26 M. Otaki and H. Goto, Optically Active Electrochromic Polymer Films from Cyclopenta [2, 1-*b*; 3, 4-*b'*] dithiophene Prepared in Chiral Liquid Crystal with Molecular Asymmetry Imprinting Polymerization, *Electrochim. Acta*, 2023, **455**, 142407.
  - 27 H. Nishide, N. Yoshioka, K. Inagaki, T. Kaku and E. Tsuchida, Poly [(3,5-di-*tert*-butyl-4-hydroxyphenyl) acetylene] and its polyradical derivative, *Macromolecules*, 1992, **25**, 569–575.
  - 28 N. Yoshioka, H. Nishide, T. Kaneko, H. Yoshiki and E. Tsuchida, Poly [*p*-ethynylphenyl] hydrogalvinoxyl and its polyradical derivative with high spin concentration, *Macromolecules*, 1992, **25**, 3838–3842.
  - 29 H. Nishide, T. Kaneko, T. Nii, K. Katoh, E. Tsuchida and K. Yamaguchi, Through-bond and long-range ferromagnetic spin alignment in a  $\pi$ -conjugated polyradical with a poly (phenylenevinylene) skeleton, *J. Am. Chem. Soc.*, 1995, **117**, 548–549.
  - 30 H. Nishide, T. Kaneko, T. Nii, K. Katoh, E. Tsuchida and P. M. Lahti, Poly (phenylenevinylene)-attached phenoxyl



- radicals: ferromagnetic interaction through planarized and  $\pi$ -conjugated skeletons, *J. Am. Chem. Soc.*, 1996, **118**, 9695–9704.
- 31 M. Takahashi, T. Nakazawa, E. Tsuchida and H. Nishide, Poly(4-diphenylammonium-1, 2-phenylenevinylene): a high-spin and durable polyradical, *Macromolecules*, 1999, **32**, 6383–6385.
- 32 M. Miyasaka, T. Yamazaki, E. Tsuchida and H. Nishide, Regioregular polythiophene with pendant phenoxyl radicals: a new high-spin organic polymer, *Macromolecules*, 2000, **33**, 8211–8217.
- 33 M. Miyasaka, T. Yamazaki and H. Nishide, Poly(3-phenylgalvinoxylthiophene). A new conjugated polyradical with high spin concentration, *Polym. J.*, 2001, **33**, 849.
- 34 A. E. London, H. Chen, M. A. Sabuj, J. Tropp, M. Saghayezhian, N. Eedugurala, B. A. Zhang, Y. Liu, X. Gu, B. M. Wong, N. Rai, M. K. Bowman and J. D. Azoulay, A high-spin ground-state donor–acceptor conjugated polymer, *Sci. Adv.*, 2019, **5**, eaav2336.
- 35 L. Huang, N. Eedugurala, A. Benasco, S. Zhang, K. S. Mayer, D. J. Adams, B. Fowler, M. M. Lockart, M. Saghayezhian, H. Tahir, E. R. King, S. Morgan, M. K. Bowman, X. Gu and J. D. Azoulay, Open-Shell Donor-Acceptor Conjugated Polymers with High Electrical Conductivity, *Adv. Funct. Mater.*, 2020, **30**, 1909805.
- 36 M. A. Sabuj, M. M. Huda, C. S. Sarap and N. Rai, Benzobisthiadiazole-based high-spin donor-acceptor conjugated polymers with localized spin distribution, *Mater. Adv.*, 2021, **2**, 2943–2955.
- 37 P. Wang, S. Lin, Z. Lin, M. D. Peeks, T. Van Voorhis and T. M. Swager, A Semiconducting Conjugated Radical Polymer: Ambipolar Redox Activity and Faraday Effect, *J. Am. Chem. Soc.*, 2018, **140**, 10881–10889.
- 38 P. Wang, I. Jeon, Z. Lin, M. D. Peeks, S. Savagatrup, S. E. Kooi, T. V. Voorhis and T. M. Swager, Insights into Magneto-Optics of Helical Conjugated Polymers, *J. Am. Chem. Soc.*, 2018, **140**(20), 6501–6508.
- 39 Z. Nelson, L. Delage-Laurin, M. D. Peeks and T. M. Swager, Large Faraday Rotation in Optical-Quality Phthalocyanine and Porphyrin Thin Films, *J. Am. Chem. Soc.*, 2021, **143**(18), 7096–7103.
- 40 H. Eimura, Y. Umetsu, H. Tokoro, M. Yoshio, S. I. Ohkoshi and T. Kato, Self-Assembled Fibers Containing Stable Organic Radical Moieties: Alignment and Magnetic Properties in Liquid Crystals, *Chem. Eur. J.*, 2016, **22**, 8872–8878.
- 41 T. Kato, J. Uchida, T. Ichikawa and T. Sakamoto, Functional liquid crystals towards the next generation of materials, *Angew. Chem., Int. Ed.*, 2018, **57**, 4355–4371.
- 42 M. Otaki and H. Goto, Helical Spin Polymer with Magneto-Electro-Optical Activity, *Macromolecules*, 2019, **5**, 3199–3209.
- 43 M. Otaki, K. Komaba and H. Goto, Synthesis of Polythiophene-Based Chiral Magnetic Block Copolymers with High Stereoregularity, *ACS Appl. Polym. Mater.*, 2023, **5**, 311–319.
- 44 M. Uchida, Y. Onose, Y. Matsui and Y. Tokura, Real-space observation of helical spin order, *Science*, 2006, **311**, 359.
- 45 J. Dong, S. Nimori, K. Kawabata and H. Goto, Induction of Helical Structure by Sesamin, and Production of Oriented Helical Polymer with Liquid Crystal Magneto-Electrochemical Polymerization, *J. Polym. Sci., Part A: Polym. Chem.*, 2017, **55**, 1894–1899.
- 46 I. Mogi, K. Watanabe and M. Motokawa, Magneto-electrochemistry with a Conducting Polymer, *Materials Science in Static High Magnetic Fields*, Springer, 2002, pp. 301–311.
- 47 D. C. Johnston, Magnetic structure and magnetization of helical antiferromagnets in high magnetic fields perpendicular to the helix axis at zero temperature, *Phys. Rev. B*, 2017, **96**, 104405.
- 48 S. Fang, M. S. Lee, D. A. Hrovat and W. T. Borden, Ab Initio calculations show why *m*-phenylene is not always a ferromagnetic coupler, *J. Am. Chem. Soc.*, 1995, **117**, 6727–6731.
- 49 S. Kato, K. Morokuma, D. Feller, E. R. Davidson and W. T. Borden, Ab initio study of *m*-benzoquinodimethane, *J. Am. Chem. Soc.*, 1983, **105**, 1791.

